Progress In Electromagnetics Research M, Vol. 57, 129–138, 2017

Adaptive Sharp Boundary Inversion for Transient Electromagnetic Data

Rui Guo[1, 2], Xin Wu[1, 2, *], Lihua Liu[1], Jutao Li[1], Pan Xiao[1, 2], and Guangyou Fang[1]

Abstract—An adaptive sharp boundary inversion scheme is developed to improve resolution with feasibility for transient electromagnetic (TEM) data inversion. By using weighted minimum gradient support (WMGS) constraint, this method focuses the resistivity change areas on layer boundary locations. Prior information describing roughness can be added into the constraint to improve resolution. Furthermore, even though no prior information about layer boundaries is available, it can still reconstruct models with geo-electrical interfaces. Synthetic models prove that this method has a better performance in presenting layer boundaries than smooth-model inversion. Field data of a TEM test line are inverted using this method, which makes the basement layer visualized easily.

1. INTRODUCTION

Transient electromagnetic method (TEM) is a powerful geophysical prospecting tool for mineral, energy and groundwater exploration as well as shallow geological investigation, etc. [1–4]. It is an artificial source electromagnetic detection method based on the process of transmitting the primary electromagnetic impulse to underground and analyzing changes of secondary field versus time to get the electrical characters of the medium [5]. The secondary field is induced by the eddy current underground, typically appearing from 10^{-6} s after the transmitting current is cut off.

Inversion is a major approach for TEM data interpretation, but it is ill-posed because of the non-linearity property of the forward modeling operator [6]. To reduce the chance of stepping into local minima, constraints of spatial resistivity are imposed on optimization functions. The most accepted constraint is the smooth model, assuming the underground resistivity changing continuously. For many years, this constraint has been applied to TEM data inversion in different methods, such as [7–9]. However, in sedimentary areas, smooth model inversion cannot reflect boundaries of the layers because it produces smooth resistivity transitions. To improve the inversion resolution in sedimentary environments, the visualization of geo-electrical interface is required. Another inversion scheme for reflecting sharp boundary is available [10–12], but it inverts resistivity and layer thickness simultaneously without parameter constraint, which makes the iteration easy to fall into local minima. Unless prior information about layer boundaries is sent into its inversion program, this method is difficult to converge.

In this work, weighted minimum gradient support (WMGS) constraint is proposed for TEM sharp boundary inversion. If there is no prior information about layer interface, WMGS constraint degenerates to minimum gradient support (MGS) [13–15] constraint, which can select the minimum volume of area where the gradient of the resistivity is nonzero. By dividing the ground into fixed dense layers, the resistivity with sharp boundary characteristics can be selected adaptively through MGS constraint to match the true resistivity distribution. If prior information about layer interface is available, the

Received 8 March 2017, Accepted 27 April 2017, Scheduled 12 June 2017

* Corresponding author: Xin Wu (wu_xin18@mail.ie.ac.cn).

[1] Key Laboratory of Electromagnetic Radiation and Sensing Technology, Chinese Academy of Sciences, Beijing 100190, China.

[2] University of Chinese Academy of Sciences, Beijing 100039, China.

proposed weight function adds geological information into inversion, which makes the layer interface to be visualized in a higher resolution.

This paper is organized as follows. In Section 2, the inverse problem models and forward modeling operations are introduced. In Section 3, the scheme of weighted minimum gradient support is explained in detail. In Section 4, the optimization problem is solved. In Sections 5 and 6, synthetic data and filed data inversion are tested to verify this algorithm. Notably, the field test was carried out by CASTEM [16] system. Conclusions follow.

2. WEIGHTED MINIMUM GRADIENT SUPPORT INVERSION

Layered model is applied here. Divide the ground into N layers with fixed thickness. Taking resolution into consideration, the thickness of the ith and $(i+1)$th layers, t_i and t_{i+1}, is better to satisfy $t_i/t_{i+1} < 1$. The resistivity of the ith layer is m_i.

The forward modeling operation can be expressed as [4]

$$H_z = \frac{Ia}{2}\int_0^\infty \lambda\left[e^{-u_0|z+h|} + r_{TE}e^{u_0(z-h)}\right]J_0(\lambda r)J_1(\lambda a)d\lambda \tag{1}$$

where:

(i) H_z is the vertical magnetic field, I the transmitter current strength, a the radius of the transmitter coil, and r the center offset between the transmitter and receiver coil. z and h are the heights of transmitter and receiver coils.

(ii) r_{TE} is the reflection coefficient noted as $r_{TE} = \frac{\lambda-\hat{u}_1}{\lambda+\hat{u}_1}$, where $\hat{u}_1$ is calculated from bottom to top using $\hat{u}_i = u_i\frac{\hat{u}_{i+1}+u_i\tanh(-2u_it_i)}{u_i+\hat{u}_{i+1}\tanh(-2u_it_i)}$, and λ is the beam of the electromagnetic wave.

(iii) u_i is called equivalent beam written as $u_i = \sqrt{\lambda^2 + i\omega\mu m_i}$ at the ith layer.

Equation (1) can be numerically calculated through fast Hankel transformations [17, 18]. The relation between theoretical data $\mathbf{d}$ and resistivity $\mathbf{m}$ can be written as

$$\mathbf{d} = F(\mathbf{m}) \tag{2}$$

where F is the forward modeling operator shorten for Eq. (1).

In practice, only observed data $\mathbf{d}_{\text{obs}}$ is available, thus we concern more about the inverse solution $\mathbf{m}$ of Eq. (2). As a property of the ill-posed problem, the inverted parameters with different distributions may have similar field characteristics [19]. To increase the stability of inversion, a reasonable constraint for inversion parameters should be imposed. One of the assumption is that parameters keep continuous in adjacent grids. This constraint is called smooth constraint, widely used in solving inverse problems. However, the continuous resistivity transitions in TEM inversion result in difficulties in distinguishing layer interfaces, hence decreasing the resolution of TEM method.

Minimum gradient support (MGS) is proposed by [13] for reflecting medium's sharp boundaries, which can be written as

$$P_{MGS} = \int_V \frac{\nabla m\cdot\nabla m}{\nabla m\cdot\nabla m+\beta}dV \tag{3}$$

where ∇ is the gradient operator in the domain V, and β is a very small positive number called focusing factor. In the ℓ_2-norm, Eq. (3) can be transformed to

$$P_{MGS} = \left\|\frac{\nabla\mathbf{m}}{\sqrt{\nabla\mathbf{m}\cdot\nabla\mathbf{m}+\beta}}\right\|_2^2 \tag{4}$$

When minimizing Eq. (4), a well-focused distribution $\mathbf{m}$ with a minimum volume of area can be adaptively selected, and the smooth distribution of $\mathbf{m}$ which results in a big value will be omitted. The results tend to have large gradient changes at layer interfaces, making blocky geological structures easily distinguished.

For prior information about layer interface to be added, Eq. (4) no longer applies. Weight minimum gradient support (WMGS) function is proposed here, written as

$$P_{MGS} = \left\| \frac{\nabla \mathbf{m}}{\sqrt{\nabla \mathbf{m} \cdot \nabla \mathbf{m} + \beta_0 \mathbf{l}}} \right\|_2^2 \tag{5}$$

where β_0 is a positive number, and $\mathbf{l}$ is the weight vector in the format of exponential function.

Suppose that a prior layer interface is located at the N_pth layer in the inversion model. Because a rough weight distribution will cause vibration of inversion results, it is reasonable to define the weight vector $\mathbf{l}$ with respect to layer n as

$$l(n) = 1 - \alpha e^{-\gamma \cdot |n - N_p - N_0|} \, (\alpha < 1) \tag{6}$$

where α and γ are used to adjust weight distribution according to prior information, and N_0 represents a constant layer number with a typical value of $2 \sim 4$. Large gradient appears at N_0 layers before low weight occurs. If no prior information is available, α is set to zero. Fig. 1 shows an example of weight distribution. In Fig. 1, suppose that the interface is at 10th layer. Let $N_p = 2$ and choose different α and γ. If it is known that there is only one interface at the 10th layer, the yellow line is suitable for weighting. If the interface number is uncertain, the red line for weighting is more conservative. However, the blue line without prior information still works, except for some resolution loss. Note that the weight is normalized, hence β_0 needs to be reselected after $\mathbf{l}$ changes.

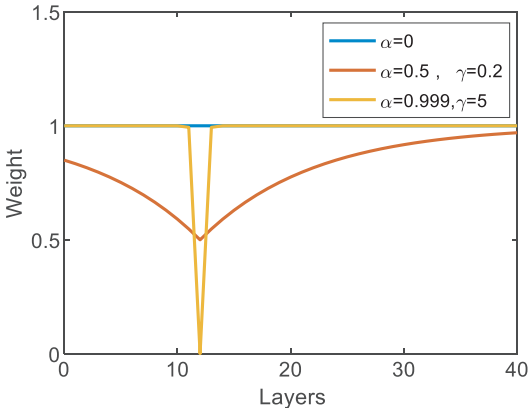

Figure 1. The weight distribution of different α and γ.

With the constraint of WMGS, the inverse problem can be faced as the solution of the following optimization scheme:

$$\min \left\| \frac{\nabla \mathbf{m}}{\sqrt{\nabla \mathbf{m} \cdot \nabla \mathbf{m} + \beta_0 \mathbf{l}}} \right\|_2^2 \tag{7}$$

$$s.t. \qquad \left\| \mathbf{W}_d \left(F(\mathbf{m}) - \mathbf{d}_{obs} \right) \right\|_2^2 < \delta \tag{8}$$

where $\mathbf{W}_d$ is the data weight, inversely proportional to the noise. Using the regularization method to form the unconstrained optimization function

$$P = \left\| \mathbf{W}_d \left(F(\mathbf{m}) - \mathbf{d}_{obs} \right) \right\|_2^2 + \lambda \left\| \frac{\nabla \mathbf{m}}{\sqrt{\nabla \mathbf{m} \cdot \nabla \mathbf{m} + \beta_0 \mathbf{l}}} \right\|_2^2 \tag{9}$$

where λ is an ad-hoc parameter [20] defining the total constraint strength.

The minimum of P can be reached when its gradient with respect to $\mathbf{m}$ vanishes. The mathematical problem can be solved by an iterative process. Suppose that there is a starting model $\mathbf{m}_0$ from which the iteration begins the refinement procedure. If F is differential at $\mathbf{m}_0$ (as we shall always assume that it is), for some sufficiently small vector $\boldsymbol{\Delta}$

$$F(\mathbf{m}_0 + \boldsymbol{\Delta}) = F(\mathbf{m}_0) + \mathbf{J}\boldsymbol{\Delta} + \varepsilon \tag{10}$$

where ε is a very small vector with the magnitude of $o\|\mathbf{\Delta}\|$, and $\mathbf{J}_0$ is an $M \times N$ gradient matrix represented as components

$$J_{ij} = \frac{\partial F_i(\mathbf{m})}{\partial m_j} \tag{11}$$

Eq. (9) can be rewrite as

$$P = \|\mathbf{W}_d(F(\mathbf{m}_0) + \mathbf{J}(\mathbf{m} - \mathbf{m}_0) - \mathbf{d}_{obs})\|_2^2 + \lambda \|\mathbf{W}_\beta \nabla \mathbf{m}\|_2^2 \tag{12}$$

with

$$\mathbf{W}_\beta \approx \mathbf{W}_{\beta 0} = \mathrm{diag}\left(\frac{1}{\sqrt{\nabla \mathbf{m}_0 \cdot \nabla \mathbf{m}_0 + \beta_0 \mathbf{l}}}\right) \tag{13}$$

By letting

$$\nabla_{\mathbf{m}} P = 0 \tag{14}$$

we have

$$2(\mathbf{W}_d\mathbf{J})^T \mathbf{W}_d [F(\mathbf{m}_0) + \mathbf{J}\mathbf{m} - \mathbf{J}\mathbf{m}_0 - \mathbf{d}_{obs}] + 2(\mathbf{W}_\beta \nabla)^T (\mathbf{W}_\beta \nabla)\mathbf{m} = 0 \tag{15}$$

After some algebra, $\mathbf{m}$ can be represented as

$$\mathbf{m} = \left[(\mathbf{W}_d\mathbf{J})^T(\mathbf{W}_d\mathbf{J}) + \alpha(\mathbf{W}_\beta\nabla)^T(\mathbf{W}_\beta\nabla)\right]^{-1} \mathbf{W}_d [\mathbf{d}_{obs} + \mathbf{J}\mathbf{m}_0 - F(\mathbf{m}_0)] \tag{16}$$

For numerical calculation, the gradient operator is written as

$$\nabla = \begin{bmatrix} 0 & & & & 0 \\ -1 & 1 & & & \\ & -1 & 1 & & 0 \\ & & \cdots & & \\ & & 0 & -1 & 1 \end{bmatrix}_{N \times N} \tag{17}$$

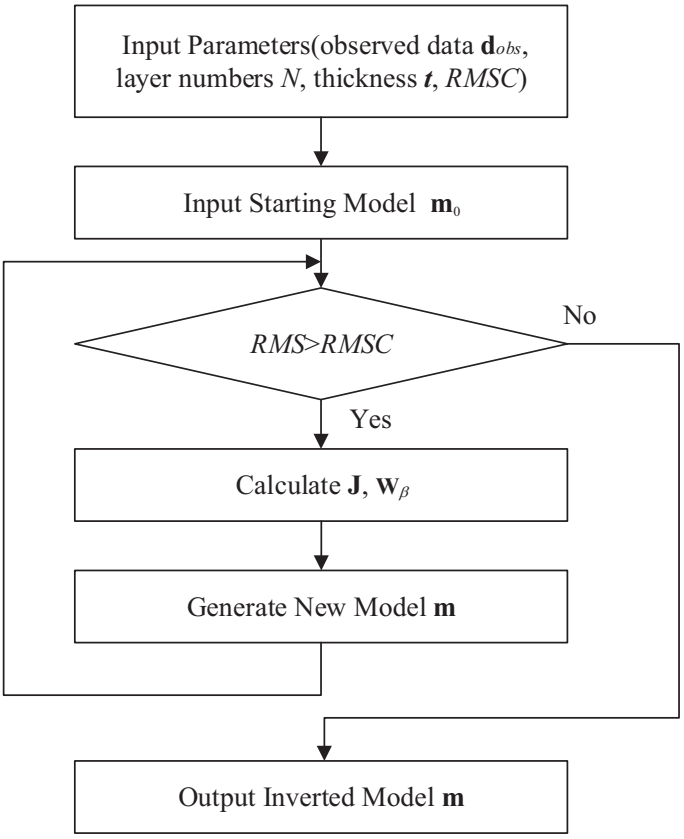

Figure 2. Inversion flowchart.

After $\mathbf{m}$ is computed, the disagreement between the forward modeling result using $\mathbf{m}$ and the real observed data can be measured by

$$RMS = \sqrt{\frac{1}{M}\sum_{V}\left(\frac{F(\mathbf{m}) - \mathbf{d}_{\text{obs}}}{\mathbf{d}_{\text{obs}}}\right)^2} \tag{18}$$

RMS should be small enough so that the forward modeling result fits observed data well. If it is not the case, $\mathbf{m}$ is then considered as the starting approximation of the next iteration. Such procedures keep on until RMS reaches an acceptable level $RMSC$. During each iteration, λ is selected using a linear searching algorithm to make sure that RMS can be as small as possible.

The inversion procedure can be represented as the flowchart in Fig. 2. In step 3, RMS is calculated by Eq. (18). In step 4, $\mathbf{J}$ and $\mathbf{W}_\beta$ are calculated by Eqs. (11) and (13). In step 5, the generated model is calculated by Eq. (16). If RMS is smaller than the level RMSC, the new model $\mathbf{m}$ can be considered as the inversion result.

3. SYNTHETIC EXAMPLES

In all the following cases, the synthetic data are simulated by means of Eq. (1) and corrupted with normalized noise with the amplitude of 0.01 nV/Am^2. The radius of transmitter coil is 100 m with the current strength 20 A. The receiver is located at the center of transmitter coil. Four models describing different underground structures are generated. Table 1 shows the parameters of these models.

Table 1. Model parameters.

Models	Resistivity (Ωm)	Thickness (m)
Model A	300	100
	100	200
	300	Half space
Model B	100	100
	300	100
	100	300
	300	Half space
Model C	300	100
	100	100
	300	200
	100	300
	300	Half space
Model D	300	100
	100 to 300	Half space

Models A, B and C are layered-models, which have clear interfaces between different layers. In model D, the resistivity increases from 100 Ωm to 300 Ωm gradually, beneath the first sedimentary layer. The responses with noises are presented in Fig. 3, which are used for inversion next. In order to provide high resolution, the ground in the inverse problem is discretized with 39 layers, with the first layer thickness 5 m and increasing ratio 1.09. The target RMS is set to 2%.

Suppose that no prior information about models A, B and C is available. In model D, prior information is that the interface is located at the 100 m underground, and we use the yellow line presented in Fig. 1 to describe the weight vector. The inversion results of WMGS are compared with that of smooth constraint inversion (see Fig. 4).

In the examples above, WMGS model inversion, represented by black lines, has larger gradient at the layer interface and is more flat in blocky areas than the smooth model inversion, represented by red

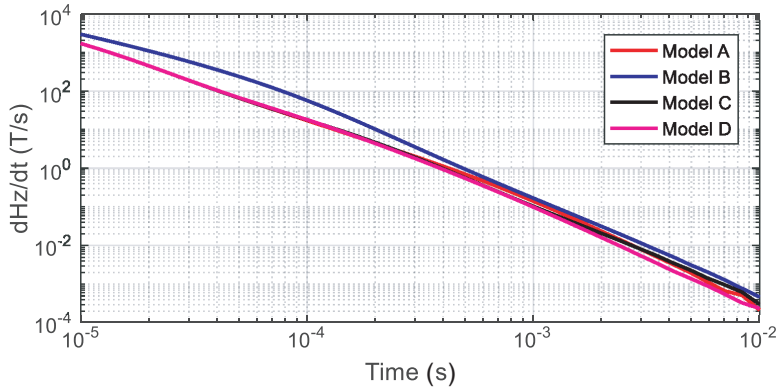

Figure 3. Responses of model A, B, C and D, with 0.01 $\mathrm{nV/m^2/A}$ noises added.

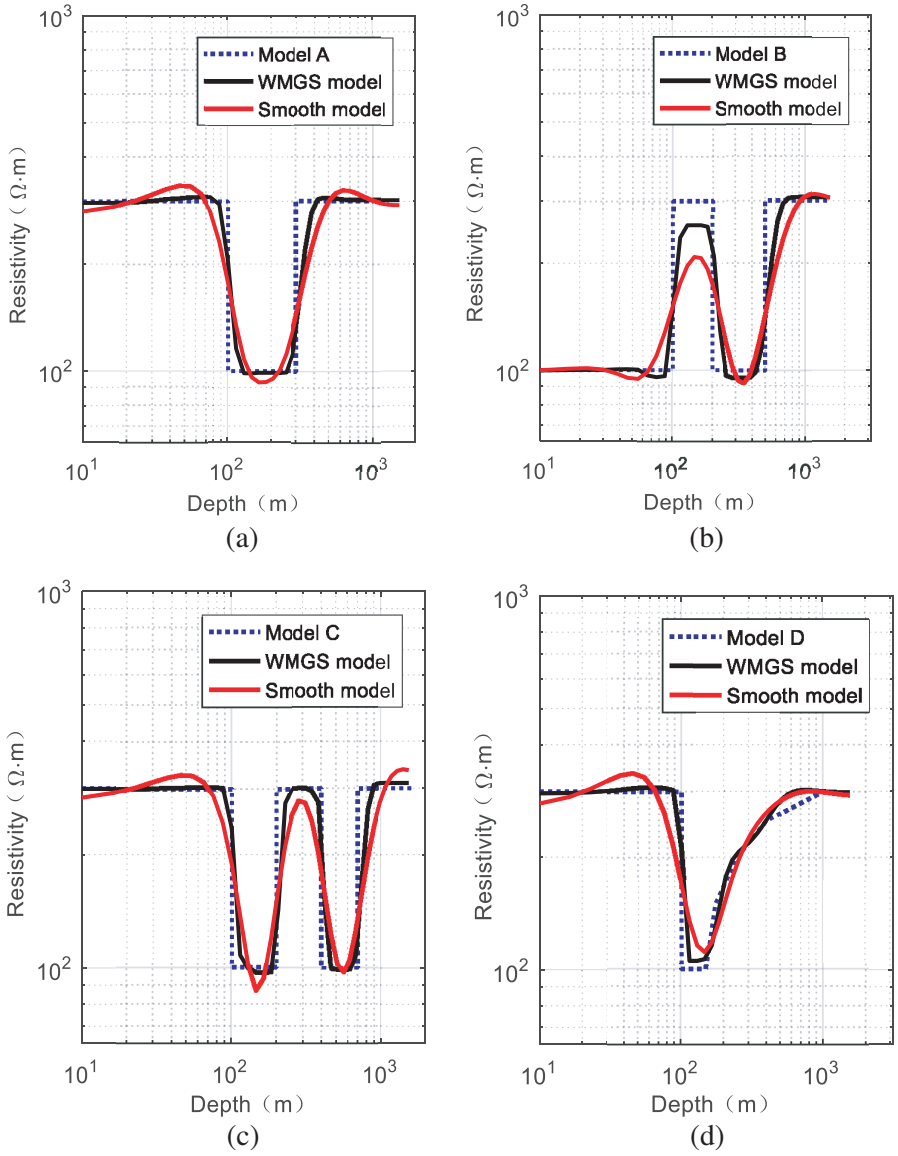

Figure 4. WMGS and smooth model inversion of (a) model A, (b) model B, (c) model C, and (d) model D.

lines. Especially in high resistivity areas, WMGS model inversion has better performance than smooth model inversion. In Fig. 4(d), WMGS can reflect both the interface at 100 m and smooth resistivity distribution beneath 100 m. It is shown that the weight (see Fig. 1) selects the model properly.

4. FIELD TEST

The field example is presented here to verify the adaptivity of this algorithm in practice. The test field is in Jianying, Anhui Province, China (see Fig. 5). According to the previous drilled results, there is a quaternary aquifer starting at 60 m underground. The test area is a typical three-layered geological structure. The thickness of the quaternary aquifer is about 400 m. At the bottom is the bed rock layer.

(a) (b)

Figure 5. Location of the field test. (a) Survey location in Jianying. (b) Jianying's location in China.

CASTEM system, developed by *Institute of Electronics, Chinese Academy of Sciences*, was used during the field test. The radius of transmitter coil is 170 m. The transmitting current is 10.8 A with the turned-off time 6 µs. More details about the system are shown in Table 2. There are 35 points along a test line. The intervals between two points is 20 m. The observed data after data processing are shown in Fig. 6.

Table 2. Parameters of CASTEM system.

Current	11.3 A
Turn-off time	$\sim$ 60 µs
Transmitting frequency	2.5 Hz
Effective areas of receiver	1000 m^2
Bandwidth of receiver	30 kHz
Number of windows	31
First window	90 µs
Last window	88.881 ms

Inversion result of a test line is shown in Fig. 7. The distance changes from 0 m to 700 m, corresponding to the test points from 1st receiver to the 35th receiver with the intervals of 20 m. From top to bottom, the resistivity distribution is high-low-high. The first part is the high resistivity

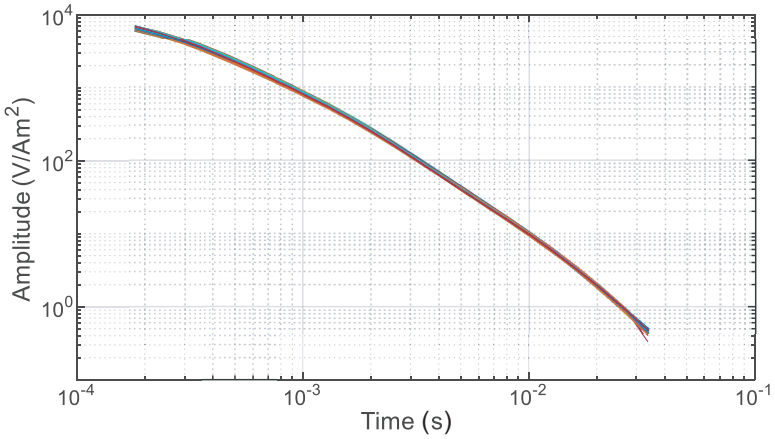

Figure 6. Observed data received by CASTEM receiver.

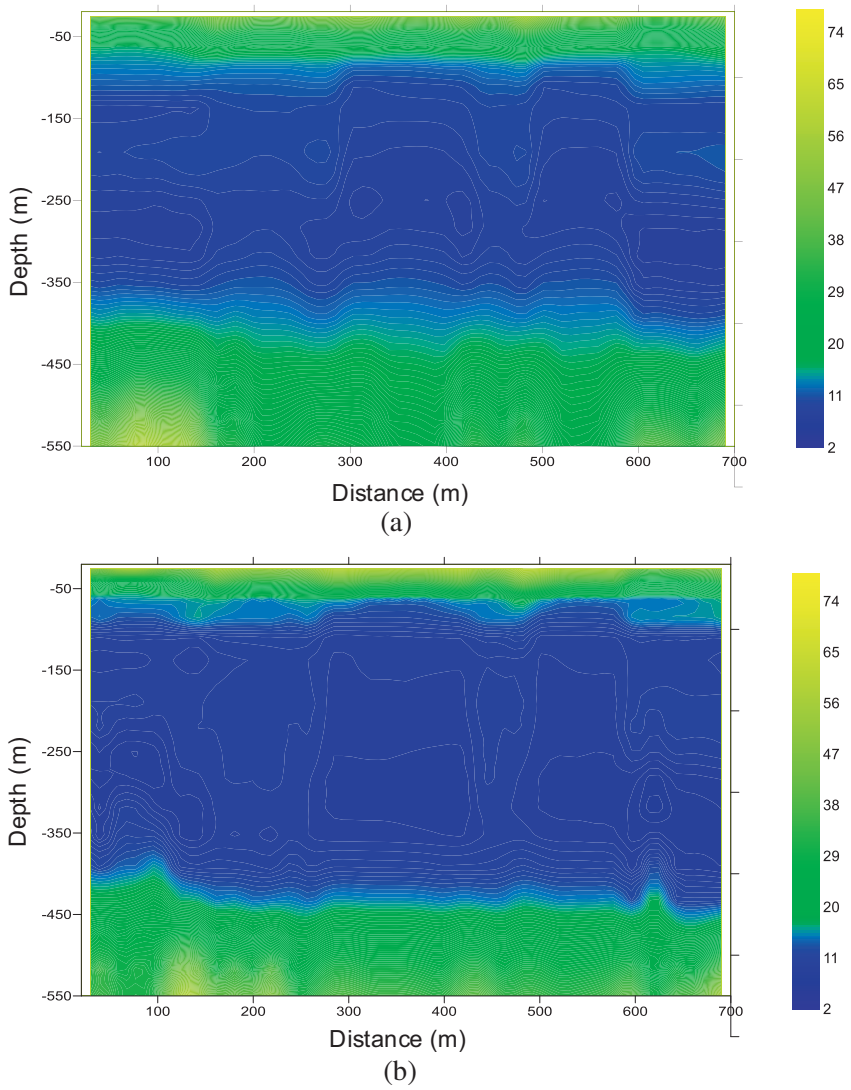

Figure 7. 2D imaging of 1D inversion. (a) Imaging using smooth model inversion. (b) Imaging using WMGS inversion.

layer at the shallow ground. At the depth of 60 m, the resistivity drops to a low level, which represents the quaternary aquifer. At the bottom is the bed rock. From Fig. 7(a) it is difficult to distinguish the interface of quaternary aquifer layer and basement layer, but Fig. 7(b) can do. It is shown that WMGS inversion has a higher resolution of the layers' interface than traditional smooth model inversion.

5. CONCLUSION

Traditional TEM inversion for sharp boundaries is easy to step into local minima, hence the smooth model inversion, which is more stable than the former, are widely accepted for data interpretation. However, in sedimentary environments, smooth model inversion has difficulties in reflecting layer interfaces, which results in the resolution loss in TEM data interpretation.

In this work, the weight minimum gradient support constraint is introduced, developed and tested. The weight is selected by a series of exponential functions according to prior information. By solving an optimization problem, the inverted images have large gradient at layer interfaces and become flatter in other areas. This inversion algorithm is tested by synthetic data, which are generated by four different models with noises corrupted. The result shows a better performance than smooth model inversion. At last, a field test is carried out by CASTEM system. After data processing, the inverted model using WMGS shows the interface between quaternary aquifer layer and basement layer with a higher resolution than smooth model inversion.

This method does not need prior information about layer interface but still makes sharp boundaries visualized adaptively. The resolution can be further enhanced by utilizing the proposed weighting scheme. It is especially applicable to inverting data observed in sedimentary areas. For areas with continuous resistivity, it is recommended that smooth model inversion is used, or the focusing factor in WMGS is large.

ACKNOWLEDGMENT

This study is supported by Chinese R&D of Key Instruments and Technologies for Deep Resources Prospecting (the National R&D Projects for Key Scientific Instruments), Grant No. ZDYZ2012-1-03-05 ATEM flight test, data process and interpretation software technology.

REFERENCES

1. He, Z., Z. Zhao, H. Liu, and J. Qin. "TFEM for oil detection: Case studies," *The Leading Edge*, Vol. 31, No. 5, 518–521, 2012.
2. Fitterman, D. V. and M. T. Stewart, "Transient electromagnetic sounding for groundwater," *Geophysics*, Vol. 51, No. 4, 995–1005, 1986.
3. Tantum, S. L. and L. M. Collins, "A comparison of algorithms for subsurface target detection and identification using time-domain electromagnetic induction data," *IEEE Transactions on Geoscience and Remote Sensing*, Vol. 39, No. 6, 1299–1306, 2001.
4. Nabighian, M., projecteditor, and J. Corbett. "Electromagnetic methods in applied geophysics, Vol. 1: Theory," *SEG*, 1988.
5. Rodi, W. and R. L. Mackie, "Nonlinear conjugate gradients algorithm for 2-D magnetotelluric inversion," *Geophysics*, Vol. 66, No. 1, 174–187, 2001.
6. Tikhonov, A. N. and V. I. Arsenin, "Solutions of ill-posed problems," *Mathematics of Computation*, Vol. 14, Winston, Washington, DC, 1977.
7. Constable, S. C., R. L. Parker, and C. G. Constable, "Occam's inversion: A practical algorithm for generating smooth models from electromagnetic sounding data," *Geophysics*, Vol. 52, No. 3, 289–300, 1987.
8. Qian, W., T. J. Gamey, J. S. Holladay, R. Lewis, and D. Abernathy, "Inversion of airborne electromagnetic data using an Occam technique to resolve a variable number of layers," *Symposium on the Application of Geophysics to Engineering and Environmental Problems*, 735–743, Society of Exploration Geophysicists, January 1997.

9. Vallée, M. A. and R. S. Smith, "Application of Occam's inversion to airborne time-domain electromagnetics," *The Leading Edge*, Vol. 28, No. 3, 284–287, 2009.
10. Smith, J. T. and J. R. Booker, "Rapid inversion of two- and three-dimensional magnetotelluric data," *Geophys. Res.*, 3905–3922, 1991.
11. Marquardt, D. W., "An algorithm for least-squares estimation of nonlinear parameters," *Journal of the Society for Industrial and Applied Mathematics*, Vol. 11, No. 2, 431–441, 1963.
12. Auken, E. and A. V. Christiansen, "Layered and laterally constrained 2D inversion of resistivity data," *Geophysics*, Vol. 69, No. 3, 752–761, 2004.
13. Portniaguine, O. and M. S. Zhdanov, "Focusing geophysical inversion images," *Geophysics*, Vol. 64, No. 3, 874–887, 1999.
14. Zhdanov, M. S., R. Ellis, and S. Mukherjee, "Three-dimensional regularized focusing inversion of gravity gradient tensor component data," *Geophysics*, Vol. 69, No. 4, 925–937, 2004.
15. Loke, M. H., I. Acworth, and T. Dahlin, "A comparison of smooth and blocky inversion methods in 2D electrical imaging surveys," *Exploration Geophysics*, Vol. 34, No. 3, 182–187, 2003.
16. Wu, X., G. Q. Xue, W. Y. Chen, et al., "Contrast test of the transient electromagnetic system (CASTEM) at the Dawangzhuang iron mine in Anhui province," *Chinese J. Geophys.*, Vol. 59, No. 12, 4448–4456, 2016, doi: 10.6038/cjg20161207.
17. Anderson, W. L., "A hybrid fast Hankel transform algorithm for electromagnetic modeling," *Geophysics*, Vol. 54, No. 2, 263–266, 1989.
18. Johansen, H. K. and K. Sørensen, "Fast Hankel transforms," *Geophysical Prospecting*, Vol. 27, No. 4, 876–901, 1979.
19. Cakoni, F. and D. Colton, *Qualitative Methods in Inverse Scattering Theory: An Introduction*, Springer Science & Business Media, 2005.
20. Hansen, P. C., "Analysis of discrete ill-posed problems by means of the L-curve," *SIAM Review*, Vol. 34, No. 4, 561–580, 1992.